A hybrid particle-polygon technique for the simulation of solid transport in a building drainage system

M.C.B. Teixeira (1), L. S. Pereira (2), R.A. Amaro Jr (3), L.Y. Cheng (4) L.H. Oliveira (5)

(1) matband@usp.br
(2) lucas_pereira@usp.br
(3) rubens.amaro@usp.br
(4) cheng.yee@usp.br
(5) lucia.helena@usp.br
(1, 2, 4, 5) Polytechnic School, University of São Paulo, Brazil
(3) Instituto de Ciências Matemáticas e de Computação, University of São Paulo, Brazil

Abstract

The steady reduction of water consumption due to sustainable provisions leads to concerns about the self-cleaning performance of building drainage networks. Moreover, the accurate prediction of complex free surface flows inside drainage pipes is particularly challenging. In a previous work, the hydrodynamics in the vicinity of a wye of a building drainage system and their influences on the solid conveyance performance were investigated through a fully particle-based modeling. Since the particle-based wall modeling of the pipe leads to more dissipative non-smooth surfaces, as a step forward on the study, a wall modeling based on unstructured triangulated surfaces associated to a polygon-to-particle contact model is adopted herein to improve the accuracy of the numerical results. The flow inside a simplified bathroom drainage system, which is represented by two drains connected by a wye to a vertical stack, is simulated considering a steady flow from a trap connected to a shower and a wash basin, and a transient flow from water closet discharge. Following the previous study, water closet discharge volumes of 4.8 and 6.0 liters (L), main drain diameters of 75 and 100 mm, and piping slopes of 0%, 1% and 2 % are considered. The computed results showed that the discharge of 4.8 L provides a better solid conveyance performance than 6.0 L, then mitigating potential issues due to clogging. In addition, the results confirm the reduction in unphysical frictional loss by using polygon-based wall modeling.

Keywords

Building Drainage System, Computational Fluid Dynamics, Particle-based Method, Moving Particle Semi-implicit, Polygon Wall Boundary.

1 Introduction

Low flush volume water closet (w.c.) has been adopted as one of the water-saving measures to alleviate the ever-growing demand on limited urban area water resources. In order to investigate the influence of the low flush volume w.c. on the self-cleaning performance of the building drainage network, numerical modeling and simulations of complex hydrodynamics inside the drains and main drains that directly receive the w.c. effluents have been conducted by using a particle-based method [1–3]. Focusing on discrete solid conveyance performance, configurations such as straight pipe and the influences of the local singularities have also been investigated [4–6].

In the author's previous work [6], the solid conveyance under the confluence flows near a wye of a drain have been studied numerically. As a result, the flow confluence at a 45º wye might deteriorate the performance and the solid might stop at the wye, showing potential for clogging, mainly in the cases featuring large diameter and zero slope. Nevertheless, as pointed by [7] unphysical frictional losses occur in the simulations of the free surface flow inside the horizontal pipes when conventional particle-based modeling of the pipe wall is adopted. As a result, flow velocity and water levels are affected by numerical model resolution. This issue resembles the additional friction due to non-smooth wall surface modeling using discrete particles.

Within this context, in the present work, following [7], the pipe wall boundaries were represented by an unstructured triangulated surface for more accurate modeling of the smoother pipes surface. In addition to this, the effects of the confluence flow on solid conveyance performance are investigated again by using a solid modeled by particles together with a polygon-to-particle contact model. Finally, the results obtained by the new numerical modeling are analyzed and the differences in relation to those obtained in the previous work [6], which is owing to smoothness of the wall modeling by particles and by polygon mesh, are also discussed.

2 Numerical model

In the present study, the fully Lagrangian meshfree moving particle semi-implicit (MPS) method, as described in [1–3], was adopted, using the free surface and solid contact models detailed in the previous works [9, 10]. However, instead of the distance of contact proposed in [10], the distance between the solid particle and the closest triangle is considered for the solid collisions. Considering a pipe flow with relatively low water level, the modeling of the air pressure oscillation due its entrapment was neglected.

Rigid pipe wall boundary

Contrary to the conventional particle wall modeling [6], the explicitly represented polygon (ERP) wall boundary technique [11], in which fixed solid walls are modeled by

a mesh of triangles, was adopted herein. In what follows, only essential formulations are presented. The reader can find more details in [8, 9].

The compact support of fluid particles near the polygon walls is not fully filled with particles. Hence, the numerical operators of these particles are divided into the contribution due fluid particles $\langle\rangle^{particle}$ and polygon walls $\langle\rangle^{wall}$, see Figure 1.

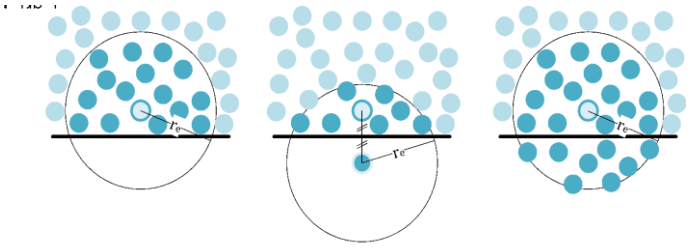

Figure 1 – Polygon wall modeling. Calculation of numerical operators with ERP model.

First, the position of the mirror particle i' corresponding to particle i is computed by:

$$r_{i\prime} = 2r_i^{wall} - r_i \,, \tag{1}$$

where r_i^{wall} is the closest point on the polygon to particle i.

Afterwards, the pressure gradient and Laplacian of the velocity, no-slip boundary condition, of the mirror particle i' are computed considering its neighbors $\Omega_{i\prime}$, and are multiplied by R_i^{ref} and the identity matrix I [11], respectively:

$$\langle \nabla P \rangle_i^{wall} = R_i^{ref} \frac{d}{pnd^0} \sum_{j \in \Omega_{i\prime}} \left(P_j + P_i - 2\hat{P}_i\right) \frac{(r_j - r_{i\prime})}{\|r_j - r_{i\prime}\|^2} \omega_{i\prime j} \,, \tag{2}$$

$$\langle \nabla^2 u \rangle_i^{wall} = -I \frac{2d}{\lambda^0 pnd^0} \sum_{j \in \Omega_{i'}} \left(u_j - u_{i'}\right) \omega_{i'j} \,. \tag{3}$$

Finally, the operators are added to the numerical operators $\langle\rangle^{particle}$ of particle i:

$$\langle \nabla P \rangle_i = \langle \nabla P \rangle_i^{particle} + \langle \nabla P \rangle_i^{wall} \,, \tag{4}$$

$$\langle \nabla^2 u \rangle_i = \langle \nabla^2 u \rangle_i^{particle} + \langle \nabla^2 u \rangle_i^{wall} \,. \tag{5}$$

The transformation matrix for reflection across the plane R_i^{ref} is expressed as:

$$R_i^{ref} = I - 2n_i^{wall} \otimes n_i^{wall} \,, \tag{6}$$

where n_i^{wall} represents the unit normal vector at the position of particle i.

The Eq. (3) represents the Laplacian of velocity for the no-slip boundary condition on a wall, here with velocity $u_i^{wall} = 0$, whose velocity of the mirror particle i' is:

$$u_{i,} = -I\{u_i - 2[u_i^{wall} - (n_i^{wall} \cdot u_i^{wall})n_i^{wall}]\}, \tag{7}$$

A repulsive force f_i^{rep} based on Lennard-Jones potential [12] is added to Eq. (15) to prevent penetrations of the fluid particles at curved edges of the mesh:

$$f_i^{rep} = \{-\frac{D_{rep}}{\|r_{iw}\|}\left[\left(\frac{0.5l_0}{\|r_{iw}\|}\right)^{n1} - \left(\frac{0.5l_0}{\|r_{iw}\|}\right)^{n2}\right] n_i^{wall} \ \|r_{iw}\| \leq 0.5l_0 \ 0 \ otherwise \ , \tag{8}$$

where $r_{iw} = r_i^{wall} - r_i$, $(n_1, n_2) = (4,2)$, $D_{rep} = \rho C_{rep}|V_{MAX}|^2$, with V_{MAX} the maximum fluid's velocity, and the repulsive coefficient $C_{rep} = 1$ are used for all simulations.

It is worth noticing that in the ERP the Neumann boundary condition for pressure is satisfied and the free-slip/no-slip condition for velocity on the walls can be applied.

3 Simplified bathroom drainage system

Following [2] and [6], the simulated model consists of two drains. Pipe 1 receives the discharge of a w.c. and the Pipe 2 connects to a trap that receives the effluent of a shower and a wash basin. Both drains are connected through a wye to a stack. Figure 2 shows the main dimensions of the simulated model along with the curves representing the flow rate over time. For Pipe 1, two diameters (75 mm and 100 mm), three pipe declivities (0%, 1% and 2%) and two discharge volumes of water (4.8L and 6.0L) were considered. The diameter of the Pipe 2 is 50 mm for all simulations. The heights of the water surface level at the sections S1 to S6, see Figure 2, were measured along the simulation.

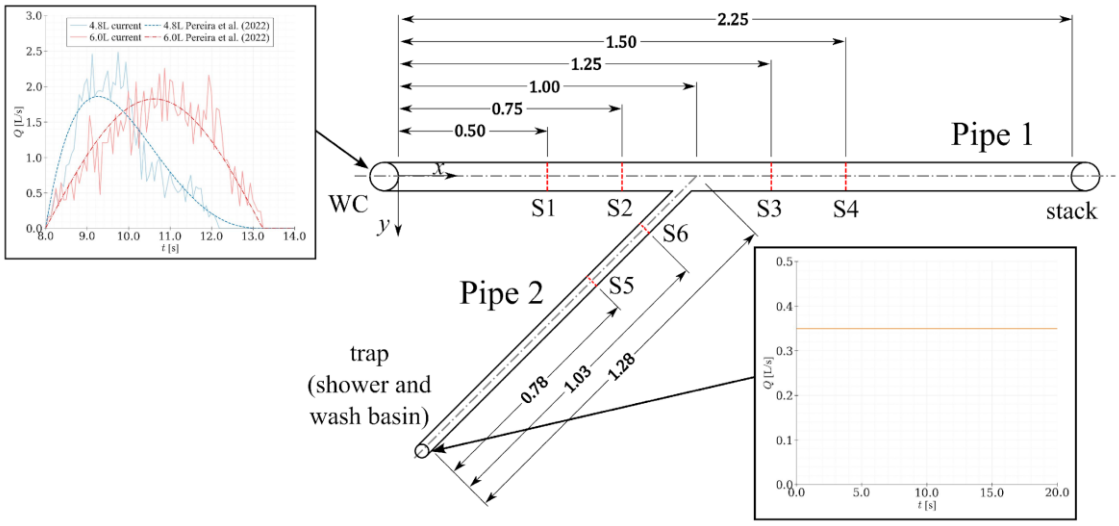

Figure 2 - Main dimensions, positions of the sensors of the simulated model (in meters). Time series of the flow rate of shower and wash basin and the w.c. flushes of the current work and of [6].

It is worth to mention that the flow rate over time of the 4.8L and 6.0L discharges, experimentally measured (solid lines), were used in the present study, while the smooth fittings (dashed lines) were used in the previous study [6].

Considering the different time scales of the flows originating from Pipe 1 and Pipe 2 (several minutes and a few seconds, respectively), the study focuses on the effects of the transient w.c. flush, while the constant flow rate from the shower of 0.35 L/s (0.2 L/s from the shower and 0.15 L/s from the wash basin) is applied as the upstream boundary condition for Pipe 2. Once the flow reaches steady state (after 8 seconds in simulations using polygon wall, and after 10 seconds using particle wall modeling [6]), the w.c. flush is discharged upstream in Pipe 1. The total duration of the simulations was 20 seconds.

The solid transport performance was evaluated by using a cylindrical-shape rigid body, six degrees of freedom (6DOF), positioned upstream of the Pipe 1 at beginning of the simulation. The material and dimensions of the solid, a cylinder of 30mm diameter and 80mm length, is based on the waste substitute of an experimental study [13]. Table 1 shows the mechanical and numerical parameters used herein.

Table 1 – Material properties and numerical parameters.

Material	Density ρ [kg/m³]	Mass m [kg]	Collision coef. ξ_n	Static friction coef. μ
Solid	1010	0.06	0.05	–
Pipe	∞	∞	–	0.22

The simulations were performed using the distance between particles of 2.0 mm and time step of $2 \cdot 10^{-4}$ s. The pressure smooth coefficient (γ) and the artificial compressibility coefficient (α) adopted were 0.01 and 10-8, respectively. For the chosen resolution, the models have approximately 600 thousand particles at their peak. Each case took approximately 16 hours to process on Intel® Xeon® Processor E5-2680 v2 2.80GHz, 10 Cores (20 Threads).

The nomenclature of the 12 simulated cases also follows that adopted in [6]), i.e., VaaDbbbAc. where "aa" is 48 or 60 and stands for the discharge volume of 4.8L and 6.0L, respectively; "bbb" is 075 or 100 denoting the pipe diameter, in mm; and "c" is 0, 1 or 2, the value of the pipe slope in %. For example, the case V48D075A0 means 4.8L discharge in 75 mm pipe at 0% slope.

4 Flow confluence at wye

Figure 3 depicts the time series of water level for all sensors (S1 to S6) for two cases V60D100A2 and V48D075A0. The position of the sensors (S1 to S6) is also shown in detail in Fig. 3b.

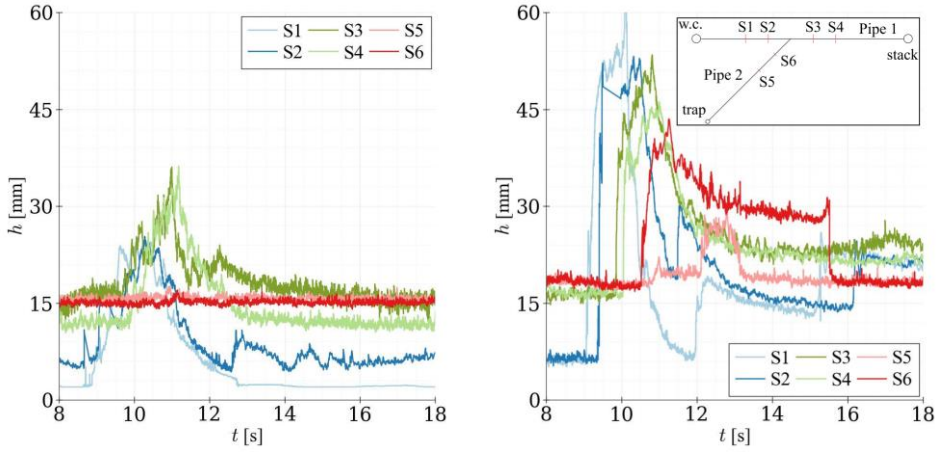

(a) V60D100A2 (b) V48D075A0

Figure 3 – Water level in the sections S1 to S6 for the cases (a) V60D100A2 and (b) V48D075A0 - without solid.

The flow from the trap which consists of the discharge of the shower and the wash basin reaches steady state at $t = 8$ s when the water level measured in the sensors located in the Pipe 2 (S5 and S6) remains constant. The water level height in both sensors S5 and S6 before the w.c. flush is approximately 15mm in V60D100A2. As expected, it is slightly lower than in V48D075A0, about 18 mm, due to larger pipe diameter and slope. After the w.c. flush discharge at $t = 8$ s, the water level in Pipe 1, S1-S4, increases.

The water level at sensor S1 in case V60D100A2 displays a single peak of about 25 mm at t=10 s, as illustrated by Fig. 3a. After the peak w.c. flush in the section, the water level inside the Pipe 1 decreases steadily to the initial condition.

From Fig. 3b, the sudden increase of water level is steeper for the case V48D075A0, and at $t = 10$ s, a peak of approximately 60 mm at the sensor S2 was computed. After a decrease in the height until near t = 12.5 s, the water level at the sensors S1 and S2, upstream the wye, rises again around t = 12.5 s and $t = 16$ s. The second and third peaks are associated with the encounter of discharged flows in the wye, leading to a backwater wave in Pipe 1 upstream to the wye. This phenomenon is more evident for the cases where Pipe 1 has smaller diameter and lower slope.

Regarding the Pipe 2, the cases V48D075A0 and V60D100A2 showed some distinct characteristics. In case V60D100A2 the water level of Pipe 2 remains unchanged during the w.c. discharge (Fig. 3a). On the other hand, from Fig. 3b, there is an increase in the water level in section S6 at t =10.6 s and in S5 at t =12 s, in V48D075A0. This is owing

to the backward wave propagation from the wye to upstream caused by the encounter of the peak w.c. flush with the steady flow at the wye. At $t = 11$ s, the sensor S6 presents a peak water level height of 43 mm. The current results in upstream sections of Pipe 2, S5 and S6, exhibit a water level peak magnitude, with shorter duration due to the w.c. flush discharge, smaller than those obtained by [6]. After $t = 16$ s, the water level in the upstream sections return to the initial level prior to the w.c. discharge.

Figure 4 presents the maximum pipe filling (dimensionless water level) in section S6 of the Pipe 2 as a function of the slope for all simulated cases. The scenarios with Pipe 1 diameter of 75 mm exhibit pipe filling higher than those with the diameter of 100 mm, in special for the null pipe slope, in which the maximum pipe filling exceeds 0.85. An increase in pipe slope leads to a decrease in the maximum pipe filling value, more evident for the cases with Pipe 1 diameter of 75 mm (V48D075 and V60D075). Furthermore, very close water levels were obtained for all cases with 1% and 2% slope.

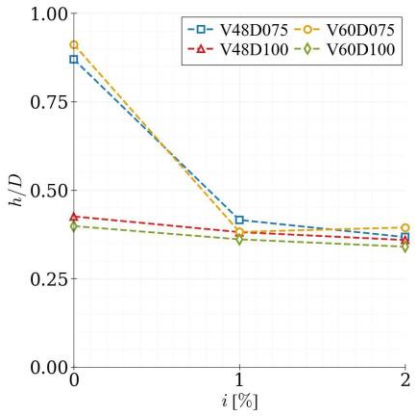

Figure 4 – Maximum pipe filling (dimensionless water level) in section S6 as a function of slope – without solid.

5 Solid conveyance near the wye

To evaluate the solid conveyance performance in the simplified bathroom drainage model, a rigid body 6DOF was initially positioned close to the upstream end of Pipe 1.

Figure 5 shows snapshots from the cases V60D075A0 and V48D100A0 with the solid. The color scale of the fluid particles represents their velocity magnitude, and the body is represented by black color. At $t = 8$ s, the w.c. flush is discharged generating a wave that propagates inside the Pipe 1.

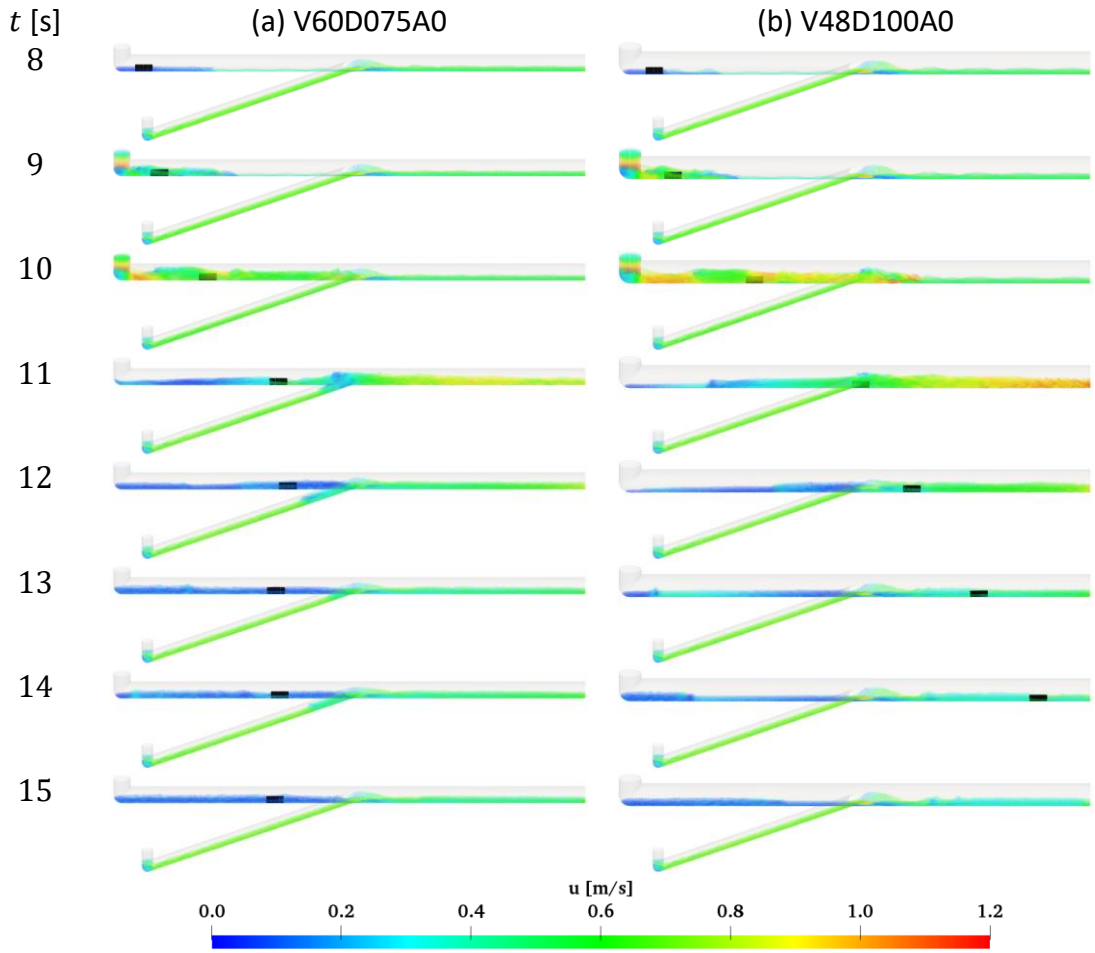

Figure 5 – Snapshots of the simulations of the cases (a) V60D075A0 and (b) V48D100A0 - with solid.

In case V60D075A0, the wavefront of the w.c. discharge hits the solid, which is abruptly accelerated and slides in contact with the pipe invert (Fig. 5a). As the solid approaches the wye, its velocity decreases due to the influence of the flow from Pipe 2. Afterwards, the solid stops at $t = 12$ s and remains deposited until the simulation's end.

In case V48D100A0 (Fig. 5b), the flow confluence near the wye decelerates the solid but is not enough to stop it, which passes through the wye at $t = 11$ s. After that, the velocity of the solid increases once again, reaching the stack before $t = 15$ s.

Despite the lower w.c. flush volume, the solid reaches the stack in case V48D100A0, while it stops before the wye in case V60A075A0. This is because the discharge of the 4.8L w.c. flush has a steeper increase of flow rate and consequently higher flow velocity that provides larger momentum transfer to the solid through the impact even when the Pipe 1 diameter is larger, as shown in Figure 5 at $t = 10$ s.

Figure 6 provides the time series for the x position of the solid within Pipe 1 across all simulated scenarios. The origin of the coordinate system of the x-axis is at the upstream (left) end of Pipe 1, as depicted in Figure 1. Before the w.c. flush discharge, the solid

slides slowly along the pipe invert for the scenarios with 1% or 2% of pipe slope. As a result, the position of the solid at $t = 8$ s varies slightly for each case.

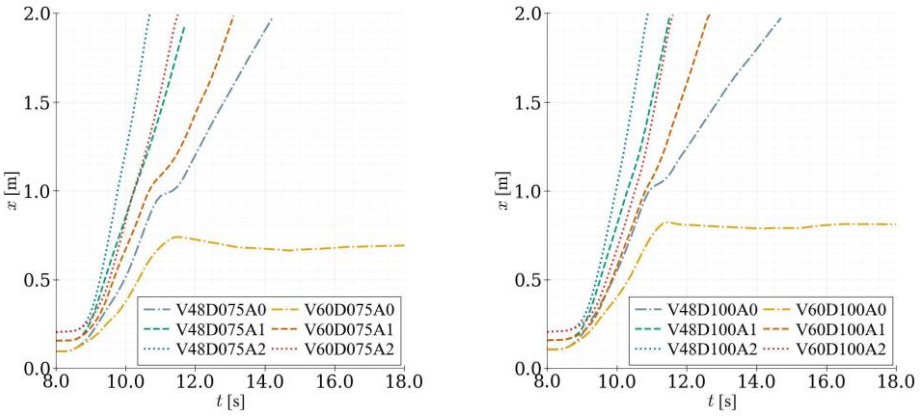

(a) $D = 75$ mm (b) $D = 100$ mm

Figure 6 – Time series of the solid position in x-axis, Pipe 1 diameter of (a) 75 mm and (b) 100 mm.

The times series exhibit a sudden increase of solid velocity due to the impact of the wavefront of the w.c. flush discharge on the solid. After that, an inflection occurs in most cases when the solid reaches the wye. Out of the 12 simulated cases, in the two (V60D075A0 and V60D100A0) with 6.0 L w.c. flush volume and null pipe slope, the solid do not reach the stack during the simulation (Fig. 6a and Fig. 6b) and remains deposited near the position $x = 0.7$ m until the simulation's end.

On the other hand, it is interesting to point out that in the other two cases with null pipe slope and flush volume of 4.8 L (V48D075A0 and V48D100A0), the solid is able to pass through the wye, although its motion is decelerated near the wye. In the other words, in the worst situation of null pipe slope, the cases with flush volume of 4.8 L, which presents steeper increase of flow rate, provide better solid conveyance performances than the cases with 6.0 L.

Figure 7 presents the comparison between the time series of solid position in x-axis of cases with null pipe slope obtained by the current study and those performed previously by [6]. From the numerical results by using the polygon-based wall modeling, the steeper increase of flush rate in 4.8 L discharge is critical for the solid conveyance through the wye. On the other hand, the results from the previous study using particle-based wall modeling, a numerical technique that induces unphysical frictional loss, the diameter of Pipe 1 is a critical factor that leads to the clogging.

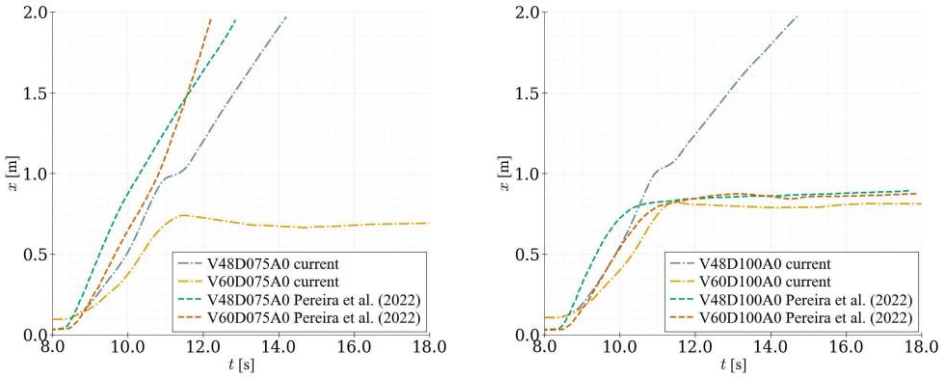

(a) $D = 75$ mm (b) $D = 100$ mm

Figure 7 – Time series of the solid position in x-axis, Pipe 1 diameter of (a) 75 mm and (b) 100 mm for the current simulations and performed by [6].

6 Final considerations

This work focused on the investigation of hydrodynamics and solid transport in a simplified bathroom drainage model considering 2 pipes: Pipe 1 receives the discharge of a w.c. and Pipe 2 connects to a trap that receives the effluent of a shower and a wash basin. 12 scenarios considering different w.c. flush volumes, Pipe 1 diameters and slopes, were evaluated. An improved modeling of wall boundary based on an unstructured triangulated mesh was adopted to represent smoother pipe surfaces.

Concerning the flow confluence on the wye, a backwater wave is generated by the convergence of the discharges in the wye and propagates upstream in Pipe 1 in the cases with smaller Pipe 1 diameter and lower pipe slope. Compared to the computed results of the former study carried out using conventional particle-based modeling of the pipe wall, the water level heights in the upstream sections of Pipe 2 exhibits a smaller peak magnitude with shorter duration due to the w.c. flush discharge flowing through the wye. These differences can be explained by the present smoother representation of the pipe wall boundary using polygons, with reduced unphysical frictional loss.

Regarding the solid conveyance, the confluence at the wye might negatively impact the solid transport performance when the pipe slope is null and the 6.0 L w.c. flush volume is adopted. On the other hand, despite the lower flush volume, the 4.8 L discharge provides better conveyance performance due to the steeper increase of flow rate. In two cases with 6.0L and 0% pipe slope, V60D075A0 and V60D100A0, the solid stopped before the wye. Reductions in solid velocity were also observed in cases with 1% pipe slope.

As future works, it is recommended to validate the numerical model through experimental results. In addition, considering the relatively high-water levels in cases with lower pipe slope, the modeling of the effect of entrapped air is recommended for further studies.

Acknowledgments

The authors would like to thank the Coordination for the Improvement of Higher Education Personnel – CAPES and University of São Paulo, respectively, for the doctoral and undergraduate research scholarships (PUB). R.A. Amaro Jr gratefully acknowledges the financial support received from the São Paulo Research Foundation FAPESP/CEPID/CeMEAI grant 2021/11429-4.

7 References

[1] L.-Y. Cheng, L. H. Oliveira, and E. H. Favero, "Particle-based Numerical Analysis of Drainage Flow inside Building System.," *International Symposium Cib W062 on Water Supply and Drainage for Buildings*, no. 1, pp. 227–238, 2012.

[2] L.-Y. Cheng, L. H. Oliveira, E. H. Favero, I. B. Oliveira, and O. M. Gonçalves, "Simulation of drainage system in building using particle-based numerical method.," in *International Symposium Cib W062 on Water Supply and Drainage for Buildings*, 2013, pp. 77–91.

[3] L. Y. Cheng, L. H. Oliveira, D. A. Ferracini, and O. M. Gonçalves, "A numerical study on waste transport in main drain," in *International Symposium Cib W062 on Water Supply and Drainage for Buildings*, 2014, pp. 1–12.

[4] L.-Y. Cheng, L. H. Oliveira, P. H. S. Osello, and Rubens Augusto Amaro Jr., "A numerical modeling of solid waste transport in main drain," in *International Symposium Cib W062 on Water Supply and Drainage for Buildings*, 2016, pp. 1–10.

[5] L.-Y. Cheng, L. H. Oliveira, P. H. S. Osello, and A. Jr. Rubens Augusto, "A numerical investigation on the hydrodynamic impact loads of the solid waste transport inside main drains," *International Symposium Cib W062 on Water Supply and Drainage for Buildings*, no. 1, pp. 463–474, 2017.

[6] L. S. Pereira, M. C. B. Teixeira, R. A. Amaro, L. Y. Cheng, and L. H. Oliveira, "Particle-based Numerical Investigation on the Hydrodynamics in the Vicinity of a Wye in a Building Drainage System," in *International Symposium Cib W062 on Water Supply and Drainage for Buildings*, 2022, pp. 433–446.

[7] L. S. Pereira, R. Amaro Junior, and L.-Y. Cheng, "The Influence of Wall Boundary Modeling on the Unphysical Frictional Loss Inside Horizontal Main Drain," 2021, pp. 1262–1275. doi: 10.1007/978-3-030-51295-8_89.

[8] S. Koshizuka and Y. Oka, "Moving particle semi implicit method for fragmentation of incompressible fluid," *Nuclear Science and Engineering*, vol. 123, no. 3, pp. 421–434, 1996.

[9] M. M. Tsukamoto, L. Y. Cheng, and F. K. Motezuki, “Fluid interface detection technique based on neighborhood particles centroid deviation (NPCD) for particle methods,” *Int J Numer Methods Fluids*, vol. 82, no. 3, pp. 148–168, 2016, doi: 10.1002/fld.4213.

[10] R. A. Amaro Jr., L.-Y. Cheng, and P. H. S. Osello, “An improvement of rigid bodies contact for particle - based non - smooth walls modeling,” *Comput Part Mech*, vol. 6, no. 4, pp. 561–580, 2019, doi: 10.1007/s40571-019-00233-4.

[11] N. Mitsume, S. Yoshimura, K. Murotani, and T. Yamada, “Explicitly represented polygon wall boundary model for the explicit MPS method,” *Comput Part Mech*, vol. 2, no. 1, pp. 73–89, 2015, doi: 10.1007/s40571-015-0037-8.

[12] R. A. Amaro Junior, A. Gay Neto, and L. Cheng, “Three-dimensional weakly compressible moving particle simulation coupled with geometrically nonlinear shell for hydro-elastic free-surface flows,” *Int J Numer Methods Fluids*, vol. 94, no. 8, pp. 1048–1081, Aug. 2022, doi: 10.1002/fld.5083.

[13] K. Akiyama, M. Otsuka, and H. Shigefuji, “Basic Study on a Method for Predicting the Waste-Carrying Performance in the Horizontal Drain Pipe of a Water-Saving Toilet,” in *CIB W062*, 2014, p. 12. Accessed: Nov. 23, 2018. [Online]. Available: https://www.irbnet.de/daten/iconda/CIB_DC27571.pdf

8 Presentation of Authors

Matheus Carlos Bandeira Teixeira is an undergraduate student in the civil engineering at Escola Politécnica of University of São Paulo, where he is performing his undergraduate research focusing on particle-based numerical simulations.

Lucas Soares Pereira is a doctor degree student in the Graduating Program in Civil Engineering, Polytechnique School of the University of São Paulo, where he is performing research on particle-based numerical simulations.

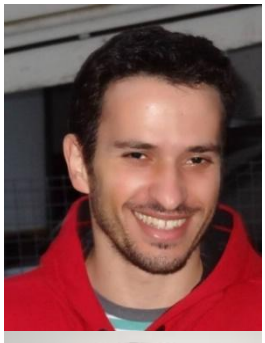

Rubens Augusto Amaro Junior is a postdoctoral fellow at the Institute of Mathematics and Computer Sciences from the University of São Paulo (ICMC-USP), Brazil. His research is related to the development of particle-based methods, including coupled solution strategies (particle-mesh), and their application to environmental fluid mechanics problems.

Liang-Yee Cheng is an assistant professor at Department of Construction Engineering of Escola Politécnica of University of São Paulo, where he teaches and conducts research on CFD modeling and simulation of fluid-structure interactions and graphic geometry for engineering and architecture.

Lúcia Helena is an associate professor at the Department of Construction Engineering of Escola Politécnica of University of São Paulo, where she teaches and conducts research work on building services.